



This paper is a part of the hereunder thematic dossier published in OGST Journal, Vol. 67, No. 1, pp. 5-178 and available online [here](#)

Cet article fait partie du dossier thématique ci-dessous publié dans la revue OGST, Vol. 67, n°1, pp. 5-178 et téléchargeable [ici](#)

DOSSIER Edited by/Sous la direction de : F.H. Nader

## Diagenesis — Fluid-Rocks Interactions

### Diagenèse minérale — Équilibres fluides-roches

Oil & Gas Science and Technology – Rev. IFP Energies nouvelles, Vol. 67 (2012), No. 1, pp. 5-178

Copyright © 2012, IFP Energies nouvelles

- 5 > Editorial
- 9 > *The Ranero Hydrothermal Dolomites (Albian, Karrantza Valley, Northwest Spain): Implications on Conceptual Dolomite Models*  
Les dolomies hydrothermales de Ranero (Albien, vallée de la Karrantza, nord-ouest de l'Espagne) : conséquences sur les modèles génétiques  
F.H. Nader, M.A. López-Horgue, M.M. Shah, J. Dewit, D. Garcia, R. Swennen, E. Iriarte, P. Muchez and B. Caline
- 31 > *Impact of Mineralogy and Diagenesis on Reservoir Quality of the Lower Cretaceous Upper Mannville Formation (Alberta, Canada)*  
Impact de la minéralogie et de la diagenèse sur la qualité des réservoirs de la Formation Mannville Supérieur, Crétacé Inférieur (Alberta, Canada)  
R. Deschamps, E. Kohler, M. Gasparrini, O. Durand, T. Euzen and F.H. Nader
- 59 > *Late Dolomitization in Basinal Limestones of the Southern Apennines Fold and Thrust Belt (Italy)*  
Dolomitisation tardo-diagénétique dans les calcaires de bassins triassiques de l'Apennin Méridional (Italie)  
A. Iannace, M. Gasparrini, T. Gabellone and S. Mazzoli
- 77 > *Empirical Calibration for Dolomite Stoichiometry Calculation: Application on Triassic Muschelkalk-Lettenkohle Carbonates (French Jura)*  
Calibration empirique pour le calcul de la stœchiométrie de la dolomite : application aux carbonates triassiques du Muschelkalk-Lettenkohle (Jura français)  
M. Turpin, F.H. Nader and E. Kohler
- 97 > *Hydrothermal Dolomites in the Early Albian (Cretaceous) Platform Carbonates (NW Spain): Nature and Origin of Dolomites and Dolomitising Fluids*  
Dolomies hydrothermales présentes dans les carbonates de la plate-forme albienne précoce (Crétacé ; NO de l'Espagne) : nature et origine des dolomies et des fluides dolomitisants  
M.M. Shah, F.H. Nader, D. Garcia, R. Swennen and R. Ellam
- 123 > *Stochastic Joint Simulation of Facies and Diagenesis: A Case Study on Early Diagenesis of the Madison Formation (Wyoming, USA)*  
Simulation stochastique couplée faciès et diagenèse. L'exemple de la diagenèse précoce dans la Formation Madison (Wyoming, USA)  
M. Barbier, Y. Hamon, B. Doligez, J.-P. Callot, M. Floquet and J.-M. Daniel
- 147 > *Impact of Diagenetic Alterations on the Petrophysical and Multiphase Flow Properties of Carbonate Rocks using a Reactive Pore Network Modeling Approach*  
Impact des altérations diagénétiques sur les propriétés pétrophysiques et d'écoulement polyphasique de roches carbonates en utilisant une modélisation par l'approche réseau de pores  
L. Algive, S. Békri, F.H. Nader, O. Lerat and O. Vizika
- 161 > *Quantification and Prediction of the 3D Pore Network Evolution in Carbonate Reservoir Rocks*  
Quantification et prédiction de l'évolution d'un réseau 3D de pores dans des roches réservoirs de carbonates  
E. De Boever, C. Varloteaux, F.H. Nader, A. Foubert, S. Békri, S. Youssef and E. Rosenberg

# The Ranero Hydrothermal Dolomites (Albian, Karrantza Valley, Northwest Spain): Implications on Conceptual Dolomite Models

F.H. Nader<sup>1\*</sup>, M.A. López-Horgue<sup>2</sup>, M.M. Shah<sup>1,3,4</sup>, J. Dewit<sup>3</sup>, D. Garcia<sup>4</sup>, R. Swennen<sup>3</sup>,  
E. Iriarte<sup>5</sup>, P. Muchez<sup>3</sup> and B. Caline<sup>6</sup>

<sup>1</sup> IFP Energies nouvelles, 1-4 avenue de Bois-Préau, 92852 Rueil-Malmaison Cedex - France

<sup>2</sup> Estratigrafia eta Paleontologia Saila, Zientzia eta Teknologia Fakultatea, Euskal Herriko Unibertsitatea,  
Sarriena z/g, 48940 Leioa, Basque Country - Spain

<sup>3</sup> Geodynamics and Geofluids Research Group, Geology Section, Department of Earth and Environmental Sciences,  
K.U.Leuven, Celestijnenlaan 200E, 3001 Heverlee - Belgium

<sup>4</sup> Centre SPIN - ENSMSE, 158 cours Fauriel, 42023 Saint-Étienne - France

<sup>5</sup> CCHS-Institución Milá i Fontanals, CSIC, Egipcíacques 15, 08001 Barcelona - Spain

<sup>6</sup> TOTAL E & P Recherche Développement, Carbonate Sedimentology Group, avenue Larribau s/n, 64018 Pau Cedex - France

e-mail: fadi-henri.nader@ifpen.fr - mikel.lopezhorgue@ehu.es - mumtazmuhammad@yahoo.com - Julie.Dewit@ees.kuleuven.be  
garcia@emse.fr - Rudy.Swennen@ees.kuleuven.be - eneko.iriarte@imf.csic.es - Philippe.Muchez@ees.kuleuven.be - bruno.caline@total.com

\* Corresponding author

**Résumé — Les dolomies hydrothermales de Ranero (Albien, vallée de la Karrantza, nord-ouest de l'Espagne) : conséquences sur les modèles génétiques** — Les modalités de gisement, la pétrographie, la géochimie et certaines caractéristiques pétrophysiques des corps dolomitiques associées aux failles dans la zone de Ranero (vallée de la Karrantza, nord-ouest de l'Espagne) sont présentées dans cette étude. Les corps dolomitiques sont encaissés dans des carbonates de plateforme déposés durant l'Albien dans le Bassin Basque-Cantabrique. Les dolomies sont formées au cours d'épisodes hydrothermaux successifs par remplacement ou précipitation – dans les vides laissés par une karstification superficielle et hypogène – et sont étroitement associées à un ensemble de failles et de fractures. La formation des dolomies est précédée et suivie par des dépôts de calcite hydrothermale. L'étude minéralogique et géochimique (XRD, ICP-MS/OES, XRF, isotopes stables et Sr radiogénique) permet de distinguer plusieurs stades de formation. Les dolomies sont ferreuses (au début) ou non-ferreuses (plus tard). Elles sont presque stœchiométriques et présentent une gamme de compositions isotopiques appauvries en  $\delta^{18}\text{O}$  (–18,7 à –10,5 ‰ V-PDB) qui témoigne de la multiplicité des stades de dolomitisation et de la température élevée des fluides (150-200 °C). La formation de ces dolomies est précédée et suivie par des stylolithisations conformes à la stratification, ce qui suggère un âge fini-Albien des circulations. La chimie des dolomies, celle des silicates authigènes associés et les relations géométriques de remplacement conduisent à postuler l'action de deux types contrastés de fluides dolomitisants. Chacun d'eux est vraisemblablement dérivé de saumures sulfatées et/ou issues de la compaction, mais ils circulent ensuite dans des environnements lithologiques distincts (silicaté riche en Fe vs carbonaté pauvre en Fe) où la réduction thermique des sulfates les fait évoluer vers des propriétés contrastées : soit vers une composition acide et ferreuse (à même de précipiter une dolomie ferreuse par remplacement de calcaire), soit vers une composition pauvre en Fe et riche en S réduit (réactifs avec la dolomie ferreuse). Les moteurs de ces circulations sont peu contraints par nos observations, mais les deux types de fluides sont visiblement drainés par les failles traversant la bordure de la plateforme et qui sont associées aux diapirs.

**Abstract — The Ranero Hydrothermal Dolomites (Albian, Karrantza Valley, Northwest Spain): Implications on Conceptual Dolomite Models** — Field characteristics, petrographic and geochemical signatures, as well as some petrophysical aspects of fault-related dolomite bodies in the Ranero area (Karrantza Valley, NW Spain) are presented in this paper. These dolomite bodies are hosted by Albian slope to platform carbonates, which were deposited in the Basque-Cantabrian Basin. Replacive and void-filling dolomite phases – postdating palaeo- and hypogene karstification – are interpreted to have originated from hydrothermal fluid pulses, and are spatially related with faults and fractures. Hydrothermal calcite cements pre- and postdate dolomitization. Mineralogical and geochemical investigations (XRD, ICP-MS/OES, XRF, stable and Sr isotopes) helped in distinguishing various dolomite and calcite phases. Dolomite phases can be grouped into ferroan (early) and non-ferroan (late). Dolomites are generally stoichiometric and exhibit a broad range of depleted  $\delta^{18}\text{O}$  values ( $-18.7$  to  $-10.5\%$  V-PDB), which advocate for multiphase dolomitization and/or recrystallization at relatively high temperatures ( $150$ - $200^\circ\text{C}$ ). The observation that bed-parallel stylolites pre- and post-date dolomites suggests that dolomitization occurred during the Late Albian regional tectonic activity and related fluid expulsions. Based on carbonate chemistry, authigenic silicate chemistry and replacement relationships, two contrasting types of dolomitizing fluids are inferred. Both arguably may have initiated as sulphate-dominated brines and/or basin compactional fluids, but they seemingly undergo sulphate reduction in contact with host rocks of contrasting compositions (Fe-rich silicate vs Fe-poor carbonate) thus evolving either to acidic and ferroan (limestone replacive) or to neutral, Fe-poor and sulfidic (Fe-dolomite replacive). Fluid drives are not well constrained by our data, but both fluid types are focused along major faults that cross cut the platform edge and are associated with diapir tectonics.

## INTRODUCTION

The Ranero area, and specifically the Pozalagua Quarry (in the vicinity of the Ranero village, NW Spain), exposes unique fault-related High Temperature Dolomite (HTD) features. The walls of the Pozalagua Quarry (Fig. 1) provide a “mega thin-section”-view whereby different petrographic aspects can be studied macroscopically. This fact has attracted several research groups to the Ranero area and its vicinity (e.g. López-Horgue *et al.*, 2010; Shah *et al.*, 2010; Kurz *et al.*, 2011; Swennen *et al.*, in press). Interest in hydrothermal dolomites is also based, at least, on two major facts:

- recent integrated studies suggest that hydrothermal dolomite exists in many forms and are likely to be far more common than previously thought (Berger and Davies, 1999; Cantrell *et al.*, 2004; Nader *et al.*, 2004; Davies and Smith., 2006; López-Horgue *et al.*, 2010; Ronchi *et al.*, 2011; Conliffe *et al.*, 2010), and
- some of the known oil and gas carbonate reservoirs consists of porous dolomites that are believed to have been affected by hydrothermal fluids – whether genetically or diagenetically (e.g. Ghawar, Saudi Arabia; Cantrell *et al.*, 2004; North field, Arabian Gulf; Sudrie *et al.*, 2006).

In the Aptian and Albian rock units of the Ramales Carbonate Platform (Fig. 2), several dolomite bodies associated with faults and fractures originated in a time of intense synsedimentary tectonic activity during the mid-Cretaceous (López-Horgue *et al.*, 2010). In the Ranero area (part of the Ramales Platform), the occurrence of good outcrops of large HTD bodies allows a detailed multidisciplinary study of an

outcrop analogue of this type of hydrocarbon reservoir rocks. Such dolomites can be considered one of the best outcrop analogues of HTD that can serve to better understand the controlling factors on hydrothermal dolomitization, the morphology of dolomite lithosomes and porosity/permeability variations (e.g., López-Horgue *et al.*, 2005, 2010; Caline *et al.*, 2006; Sudrie *et al.*, 2006; Schröder *et al.*, 2008, Dewit *et al.*, 2009, 2010), which are all matters of prime interest in oil and mineral resources exploration and production.

The aim of this paper is to present the sedimentary and diagenetic aspects of the Ranero dolomites by compiling results from different research groups that have been working in this area for several years (refer to Acknowledgments). First, a review on the geological settings including the stratigraphic and structural factors, which are believed to have played important roles in the resulting dolomitization, is provided. Then, results of detailed petrographic and geochemical analyses are used in order to characterize the different diagenetic phases – a necessary step for constructing a generalized paragenetic sequence. The petrophysical properties of these dolomites have been assessed and presented with respect to the dolomite textural properties and position in the dolomite geobody. Finally, some ideas related to the dolomitizing fluids and mechanisms for their circulation and subsequent diagenetic impact are inferred.

## 1 GEOLOGICAL SETTING

The studied area, near the village of Ranero, is located in the provinces Biscay and Cantabria in northern Spain, at the

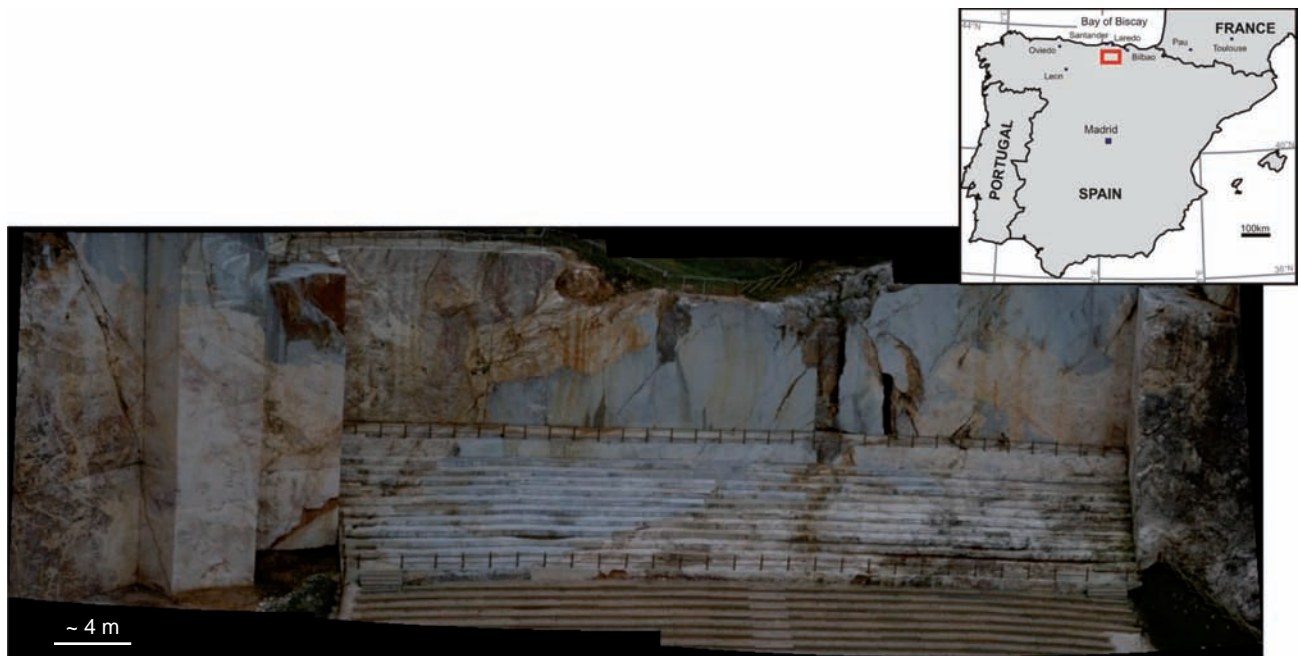


Figure 1

A panoramic view of the Pozalagua Quarry (Ranero, NW Spain) with world-class exposure of hydrothermal dolomites (index map for location of the Ranero study area).

western margin of the now inverted Basque-Cantabrian Basin (BCB). Hydrothermal dolomites are common in the BCB and typically crop out along major faults. In the area of Ranero and its surroundings, HTD are hosted in Early Albian limestones and, to a lesser extent, in Aptian and Late Albian limestones.

### 1.1 The Basque-Cantabrian Basin (BCB)

The geodynamical evolution of the BCB is directly linked to extensional tectonics related to the opening of the North Atlantic Ocean and the displacement of the Iberian plate with respect to the European plate (Boillot and Malod, 1988; Vergés and García-Senz, 2001) leading to the opening of the Bay of Biscay (Triassic-Early Cretaceous; *Fig. 2-4*). Rotation of Iberia led to geodynamical changes in the BCB with alternation of rifting and strike-slip regimes (*e.g.* Vergés and García-Senz, 2001). The BCB originated upon the onset of the Permian-Triassic boundary in which rifting subsidence led to the development of thick continental successions on the margins. Jurassic times provided a relative quiescence stage with a less active subsidence and development of marine carbonate ramps with minor thickness changes. At the end of the Jurassic and earliest Cretaceous, a main rifting phase began with a continental rift fill that was followed by the deposition of marine successions on faulted blocks during

the Aptian and Albian times. The highest subsidence in the BCB is related to cortical extension trending NE-SW and NW-SE with the development of transtensive faults during the Aptian and Albian (*e.g.*, García-Mondéjar *et al.*, 1996, 2004b). The Ranero area is characterized by E-W trending extensional faults that acted as sinistral shear faults mainly during mid Cretaceous (*Fig. 2*). During Albian-Santonian times, Iberia drifted southwestward along NW-SE strike-slip faults. The Late Cretaceous-Palaeogene interval is characterized by a widespread thermo-tectonic subsidence and the development of extensive marine depositional systems. Inversion of the BCB took place from late Eocene to early Oligocene times. The inverted BCB is the western branch of the Pyrenean folded chain. The study of the sedimentary successions (*e.g.*, thickness variations, facies changes, sedimentary offsets) and preserved kinematic indicators has permitted the reconstruction of the synsedimentary fault activity (López-Horgue *et al.*, 2010).

The BCB records a thick sedimentary succession, which is up to 14 km in the most subsiding areas – in the middle of the Basin – and dominated by Mesozoic rocks. Important synsedimentary fault activity during the Aptian and Albian led to differential subsidence. Some of the major synsedimentary faults in the BCB area are the E-W trending Cabuérniga Fault to the south of the Ranero area, the NW-SE trending Bilbao and Ruahermosa Faults to the north of the

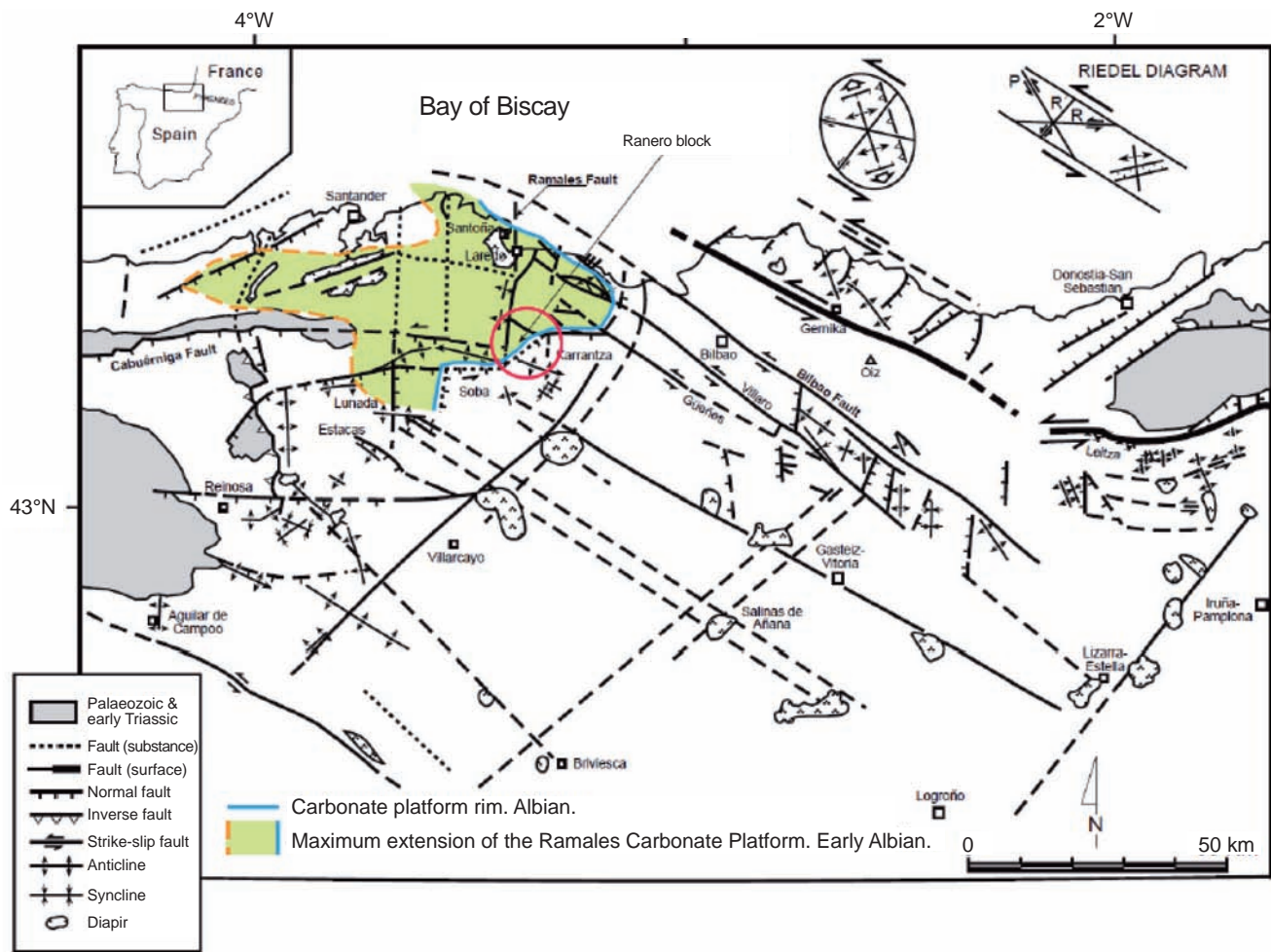


Figure 2

Synsedimentary structures of the Basque-Cantabrian Basin (BCB) during Aptian-Albian times. No palinspastic restoration. Modified from García-Mondéjar *et al.* (2004b).

Ranero area and the N-S trending Ramales Fault that connects the former ones (Fig. 2, 5; e.g. López-Horgue, 2000). These faults had a strike-slip motion at least during the Aptian and Albian when shallow marine carbonate sedimentation took place on footwall highs. The carbonate platform sedimentation changed abruptly towards deeper marine siliciclastic sediments on hanging walls, which formed troughs. Accordingly, the area between the Cabuérniga and Bilbao Faults was a large-scale structural high that controlled the development of the Ramales Carbonate Platform (e.g., García-Mondéjar *et al.*, 2004a) (Fig. 2, 3). This platform extended around 60 km southwesterly from the platform margin that follows the trend of the main strike-slip faults and of minor faults trending NNE-SSW (Fig. 2), from which there was a facies change to deeper marine siliciclastic successions to the east (Fig. 3, 4).

The Ramales and related faults are the main faults in the study area, with which dolomitization is associated; they cut across the platform margin and interior in the Ranero overstep between the Ruahermosa and Cabuérniga Faults (Fig. 5). Diapirism of Triassic evaporites is also related to the activity along these main faults (Fig. 4a, 5).

## 1.2 Stratigraphy of the HTD Host

The Ramales Platform is the largest carbonate platform that developed in the BCB, it hosts several HTD bodies such as the Ranero Body. Along the N-S trending Ramales Fault the Asón River incised a considerable sedimentary succession (Fig. 4a). In total more than 3 000 m of Triassic to Turonian strata are now exposed – 1 100 m of this succession correspond to the Aptian-Albian host limestones (López-Horgue

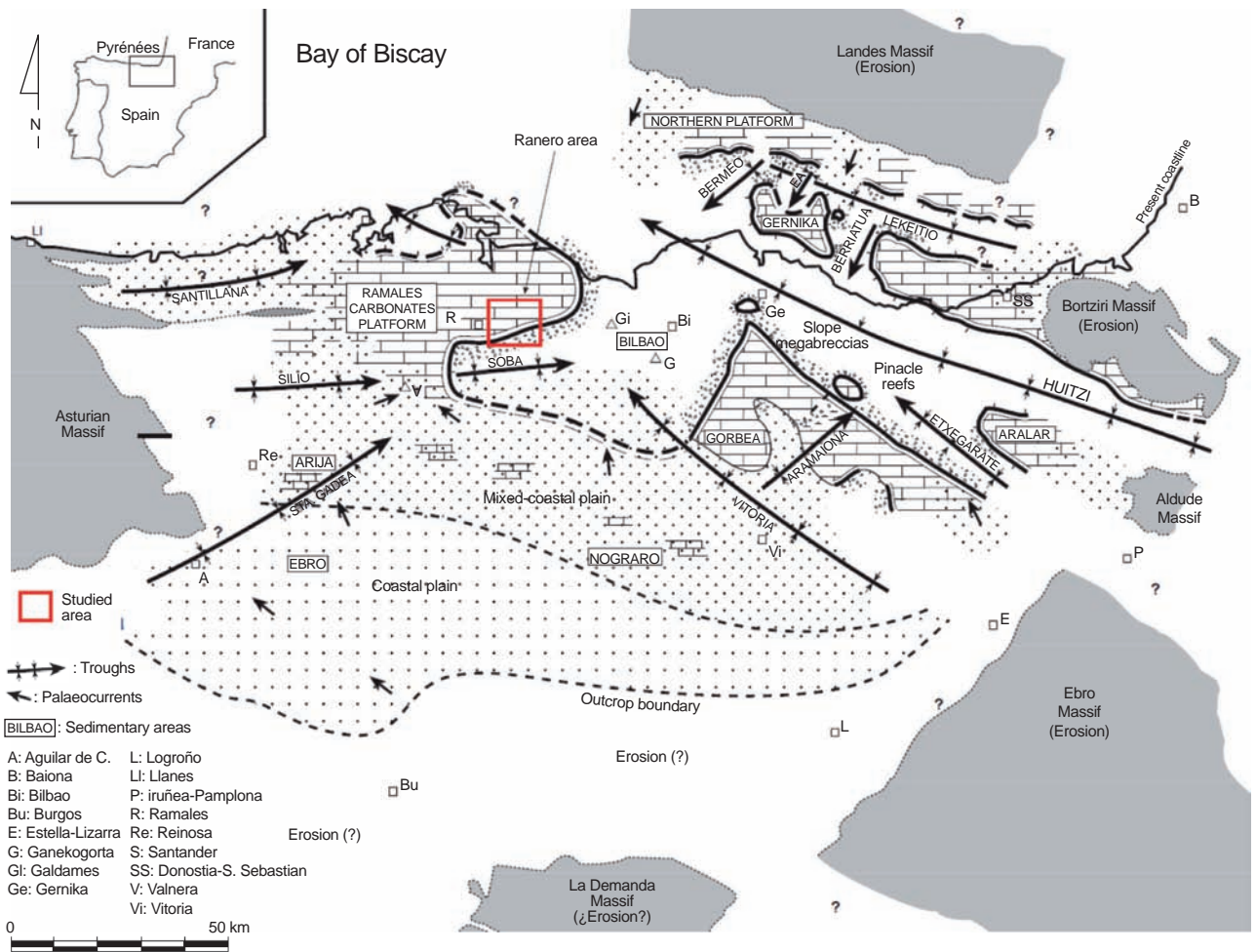


Figure 3

Paleogeographic map of the Basque-Cantabrian Basin (BCB) during Early Albian times. Studied area is highlighted. Modified from García-Mondéjar *et al.* (2004b).

*et al.*, 2010). Aptian successions are totally eroded to the east of the Rames Fault, in the Ranero area, where an angular unconformity separates Valanginian sandstones and the Early Albian limestones (López-Horgue *et al.*, 2010). Aptian-Albian limestones of the Rames Carbonate Platform, show four sedimentary stages separated by regional unconformities (López-Horgue, 2000; López-Horgue *et al.*, 2009a; Fig. 4b):

- 1 Aptian ramp;
- 2 earliest Albian distally steeped ramps;
- 3 late Early Albian to earliest Late Albian rimmed platform with steep clinofolds transitional to resedimented deposits and deep marine siliciclastics;
- 4 late Albian calcarenitic ramp with a micritic-mound belt facing shallow marine siliciclastics.

Angular unconformities between stages 1-2 and 3-4 are related to subaerial exposures and testify of the syndimentary

fault activity in the area (López-Horgue *et al.*, 2010). The unconformity between stages 2 and 3 is an erosive surface probably related to a tectonic-subsidence change in the area that conditioned the transition from ramp to rimmed platform and the inception of the deepening of the basin easterly adjacent to the carbonate platform (*e.g.*, García-Mondéjar *et al.*, 2005). A drowning event affected the Rames Platform in the middle Late Albian leading to the termination of the platform and the initiation of a shallow marine muddy sedimentation (López-Horgue, 2000). Stage 3 is divided by one of the main unconformities of the BCB associated with a hiatus comprising the Middle Albian in shallow platforms (*e.g.*, López-Horgue *et al.*, 2000) and a relatively thin sedimentary record of the basal Middle Albian in the deeper troughs. Carbonate sedimentation was mainly micritic with development of carbonate microbial mounds in the reef margin and

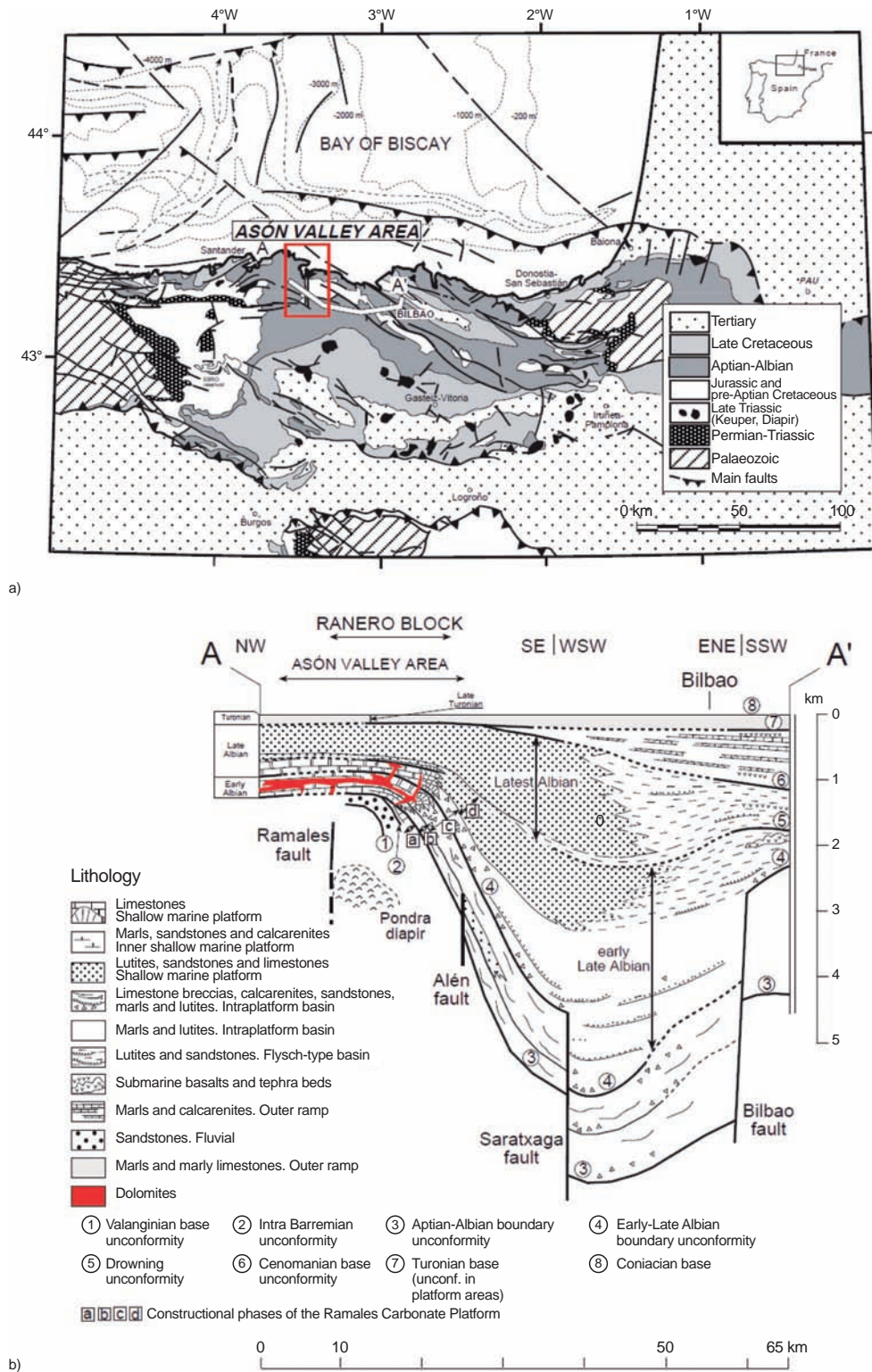


Figure 4

a) Simplified geological map of the Basque-Cantabrian Basin. The studied area lies within a zone where main structures and faults show a strike change from NW-SE to W-E. A-A' indicates the strike of b). b) Stratigraphic cross-section of the Valanginian-Turonian interval in the palaeogeographical area of the Albian Ramales Carbonate Platform and its correlative subsiding basinal area to the East. The main dolomite host is the Early Albian limestone unit. No palinspastic restoration.



Figure 5

Main tectonic structures from the study area showing an arrangement due to a syndepositional strike-slip play. The thick lines (faults) and fold-axis represent main structures that controlled the dolomitization process. The main dolomite bodies are represented in red colour. Ruahermosa and Cabuerniga Faults generated an overstep on the eastern block of the Rameses fault.

overall early diagenetic lithification (López-Horgue, 2000). Unconformities and early syndepositional fractures affecting limestones involve diagenetic alteration features such as dissolution, meteoric cementation and alteration of the marine cements (López-Horgue *et al.*, 2010).

## 2 METHODS

Aerial photographs helped in delineating dolomite bodies, which were later ground-mapped in the field (*see Fig. 6, 7*).

Sampling was carried out in the host limestone as well as across the dolomite bodies. Rock slabs and thin sections were stained with Alizarin Red S and potassium ferricyanide to differentiate ferroan from non-ferroan dolomite and calcite (Dickson, 1966). Petrographic studies of 260 thin sections were carried out using conventional (Nikon ECLIPSE LV 100 POL) and cathodoluminescence microscopy (Cathodyne OPEA; operating conditions were 12 to 17 kV gun potential, 350 to 600  $\mu$ A beam current, 0.05 Torr vacuum). Scanning Electron Microscope (SEM) equipped with an energy dispersive detector (EDX) was used for detailed observations and qualitative

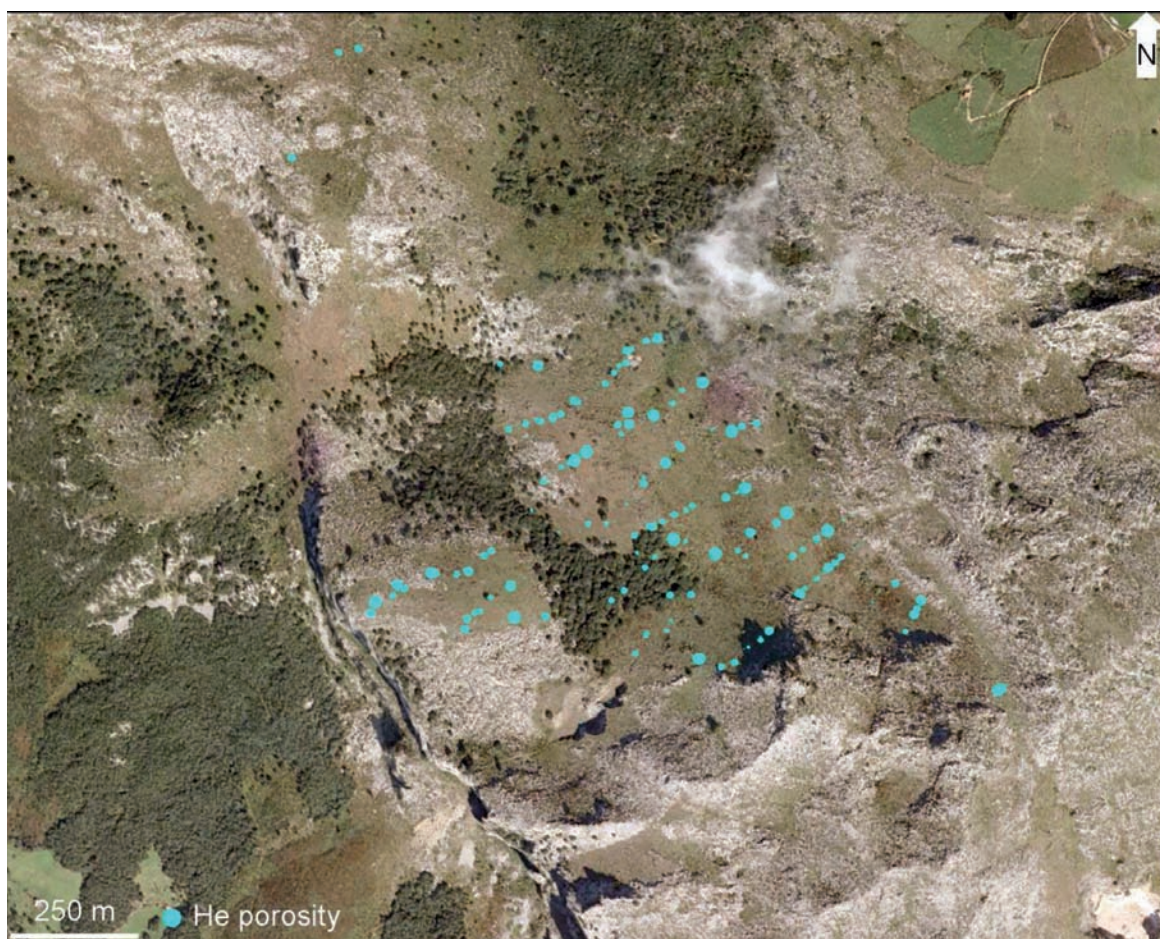


Figure 6

Spatial distribution of helium porosity values of the Pozalagua (Ranero) HTD Body. The smallest and largest circles correspond to 1.8% and 12.1% porosity, respectively.

chemical analyses at École des Mines, Saint-Étienne. Operation conditions were 12 kV beam voltage, 10 mm Working Distance (WD).

Geochemical analyses of the selective rock phases and whole rock samples were obtained by means of X-Ray Fluorescence (XRF) and Inductively-Coupled Plasma Optical Emission Spectrometry (ICP-OES) depending on the amount of material available from micro-drillings and/or plugs. All samples (250) were analysed by ICP-OES, and 128 samples by XRF in École des Mines, Saint Étienne. XRF analysis was performed with a SRS3400 spectrometer, using glass discs/pressed pellets for major/trace elements, respectively. ICP-OES analysis is performed on a JI Activa sequential device using acid solutions prepared by HF digestion. Both analytical routines are calibrated against geostandards. Coupling these techniques is effective in overcoming the

main drawback of each one, *i.e.* sensitivity for minor and trace elements by XRF (below 0.1% and 10 ppm) and reproducibility by ICP-OES (5%).

Stable isotope analyses ( $\delta^{18}\text{O}$  and  $\delta^{13}\text{C}$ ) of 275 selected samples of different dolomite types, calcite cements and the host limestone were carried out in the Department of Geology – University of Erlangen (Germany) and the Département Géologie – Jean Monnet Université (Saint-Étienne, France). All stable isotope values are reported in per mil (‰) relative to the Vienna Pee Dee Belemnite (V-PDB). The dolomite isotopic composition values are corrected by fractionation factors given by Rosenbaum and Sheppard (1986).

In the Ranero HTD body, 270 plug samples were collected in sections perpendicular and parallel to the Pozalagua Fault as well as randomly. Some 120 plugs were selected for standard helium porosity and Klinkenberg permeability measurements.

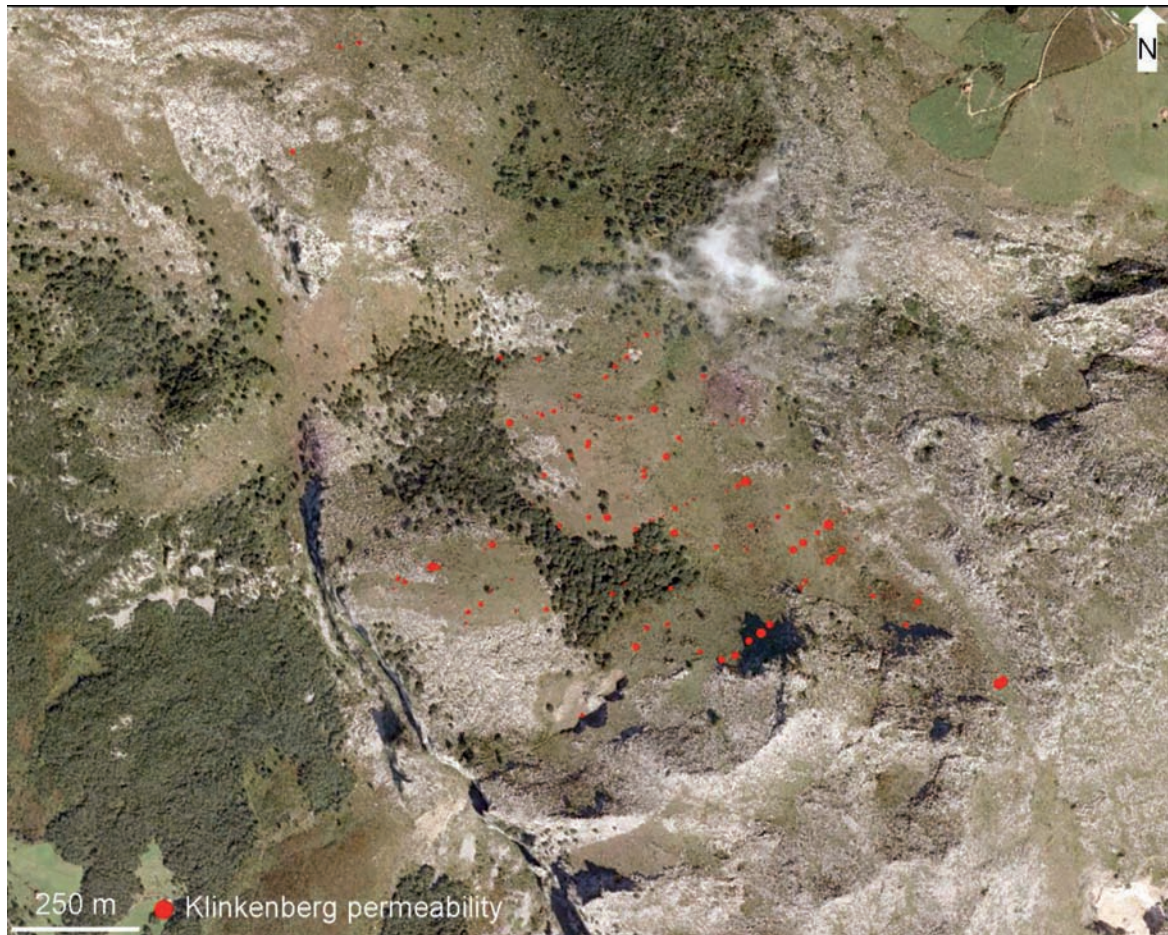


Figure 7

Spatial distribution of Klinkenberg permeability values of the Pozalagua (Ranero) HTD Body. The smallest and largest circles correspond to 0.01 mD and 17.4 mD permeability, respectively.

### 3 ANALYTICAL RESULTS

#### 3.1 Field Observations

Dolomites and Albian host limestone crop out in several sites (e.g. Ranero, Breñas, Asón estuary; *Fig. 5*). Particularly in the surroundings of Matienzo (situated west of the Breñas massif), the Aptian limestones host a HTD body of a considerable size. The origin of the HTDs is related to the same faults and they have similar paragenetic sequences (López-Horgue *et al.*, 2010). In the Ranero area an angular unconformity separates gently dipping (10-30° to the NE) Albian carbonates from underlying Valanginian to Aptian sedimentary units. This early Albian angular unconformity corresponds to the almost complete erosion of the underlying Aptian carbonates. Where preserved in the Ranero area, these

Aptian carbonates contain small patches of dolomite close to the Albian basal unconformity. Furthermore, a drowning unconformity separates the Albian limestones from younger Albian siliciclastics.

The Ranero area is the eastern structural block of the hydrothermal dolomitization system that shows characteristics of an overstep between the E-W trending Cabuérniga and Ruahermosa Faults (*Fig. 5*). Important structures of this overstep are NW-SE trending extensional faults and fractures, of which the main fault is the dolomitized Pozalagua Fault. The offset of the platform margin along the Pozalagua Fault indicates a left-lateral movement (Dewit *et al.*, 2009).

A large dolomite body expands laterally – nearly parallel to the bedding – along the Pozalagua Fault (trending NW-SE); its width increases upwards considerably in the upslope platform rocks. The dolomite body is up to 2 km wide in the

north-western part of the Ranero plateau (platform), and has a minimum thickness of ca. 500 m along the Pozalagua Fault (slope) (check Fig. 6, 7; refer to Shah *et al.*, this volume). The Pozalagua Fault dolomite facies (and textures) display a complex polyphase dolomitization history (several phases of dolomites are observed in the Pozalagua Quarry, cf. Fig. 1). Besides, their characteristic geometries (irregular, strata-discordant, fronts dying out away of the major fault; cf. Nader *et al.*, 2004, 2007) may suggest that the fault was a hydrothermal fluid-conduit.

Detailed mapping permits the identification of different fracture-related dolomite bodies, ranging from millimetre-wide dolomite-filled joints and decimetre-size pockets, to kilometre-scale large bodies. Such large dolomite bodies (Fig. 8a) are often associated with calcite dyke-like features (in the lower end of the dolomite body featured in Fig. 8a), cross-cutting basin-sediments (calciturbidites) (Fig. 8b). The dolomite/limestone contacts are easily observed in the field due to the colour contrast (beige/brown for dolomite; light grey for limestone), besides they seem to be parallel to  $S_1$  joint set in the limestone (Fig. 8c).

The structural elements associated to the dolomites have been observed during fieldwork, such as joints and pores arranged along  $S_1$  planes (Fig. 8d). All fractures in the Ranero area cut across the Albian host limestone stratification at right angles extending from foreereef to reef margin and inner platform facies and show shear-kinematic indicators (Fig. 8e, f).

Since the dolomite body extends from distal slope to reef margin and inner platform carbonates the fracture system that controls the HTD occurrence is predominantly independent of the limestone facies. The dolomite bodies in the Rmales Platform developed along main fault-zones (e.g. Pozalagua Fault and Rmales Fault) and expand laterally in their upper part forming large almost tabular bodies nearly parallel to bedding. Dolomite body boundaries follow joint planes (Fig. 8c) or show gradual rapid change to the host limestone. In the Pozalagua Fault zone dolomitization is fabric destructive. Several dolomitization phases can be distinguished according to a complex arrangement of replacement and cementation features that have different fabrics, *i.e.* including hydrofracturation, breccias and dolomite cements (preferentially) occurring along fractures enhanced by dissolution.

Away from the fault zone, the dolomites show some primary sedimentary structures; e.g. preserved bioclasts. In both fault zones and areas away from the fault-zones, decimetric-scale zebra dolomites are present, predominantly brecciated and irregular in fault-zones and subparallel to stratification away from fault zones. The origin of zebra dolomite is related to shear stresses mainly in two different structural directions: along fracture shear-corridors (López-Horgue *et al.*, 2009b) and flexural-slip bands nearly parallel to bedding (Iriarte *et al.*, 2009). Besides, some zebra dolomite clasts look very

similar to fragments of corals and may have been formed by mimic replacement of the latter (cf. Nielsen *et al.*, 1998).

### 3.2 Petrography and Geochemistry

The excellent exposures in the Pozalagua Quarry provide a survey of the main lithology types and invaluable geometrical relationships between successive stages of brecciation and calcite/dolomite precipitation and/or replacement. The present petrographic and geochemical study covers typical members of the hydrothermal sequence described by Swennen *et al.* (in press) in the Pozalagua Quarry together with samples collected in a systematic way along multiple sections across the main dolomite body and another vein body (“satellite”), one kilometre eastward (cf. Fig. 8a). This hydrothermal sequence is part of the complete diagenetic sequence proposed for the Albian host limestone and its hydrothermal dolomites of the Asón Valley area described in López-Horgue *et al.* (2010).

#### 3.2.1 Petrographic Attributes

This section is not intended to present the full details of petrographic analyses, but to only describe the sequence of diagenetic events that are significant to the objectives of this study. For additional data on the petrographic characteristics of these dolomites the readers are referred to Shah *et al.* (this volume) and López-Horgue *et al.* (2010). The Albian limestones, which are exposed in the study area, display a complex diagenetic history at regional scale (López-Horgue *et al.*, 2010; Rosales and Perez-García, 2010). Early and burial diagenetic cements (cathodoluminescence zones Z1-Z7, cf. Rosales and Perez-García, 2010) are basically fabric sensitive. Diagenetic phases associated with hydrothermal fluids are essentially fabric destructive at the grain scale and developed along NW-SE trending fracture systems. They generated both replacive dolomites and cements.

Hydrothermal cements fill the remaining void space resulting from the combination of fracturing, palaeokarst development and hydrothermal enlargement of former cavities. The sequence of hydrothermal precipitates is illustrated in Figure 9; it starts with zone Z8 of Rosales and Perez-García (2010) and occurs after phase 17 of López-Horgue *et al.* (2010), including the following phases in chronological order:

- coarse crystalline calcite is found as symmetrical fracture- or cavity-linings (Fig. 9a), in two substages:
  - a centimetre-scale palisade with a prominent chevron growth zoning (CC-I);
  - coarse crystalline calcite up to several centimetres displaying neither apparent zoning nor preferred orientation (CC-II);
- ferroan dolomite cements (CCD-I) display a characteristic banding (sub-stages) with alternating layers of variable colour (white, brown, grey) and Fe contents that line large cavities (Pozalagua Quarry) or vein walls (Fig. 9b, c). These



Figure 8

Photographs of the Ranero dolomite vein-body. a) View of the upper part of the dolomite body; b) Calcite dyke-like features in the lower end of the dolomite body, cross-cutting basin-sediments (calciturbidites); c) Dolomite/limestone boundary (parallel to S<sub>1</sub> joint set); d) Jointed dolomite with pores arranged along S<sub>1</sub> planes forming a protozebra texture; e, f) Small scale en echelon shear-joints filled with saddle dolomite, disposed in the fringe of the main dolomite body.

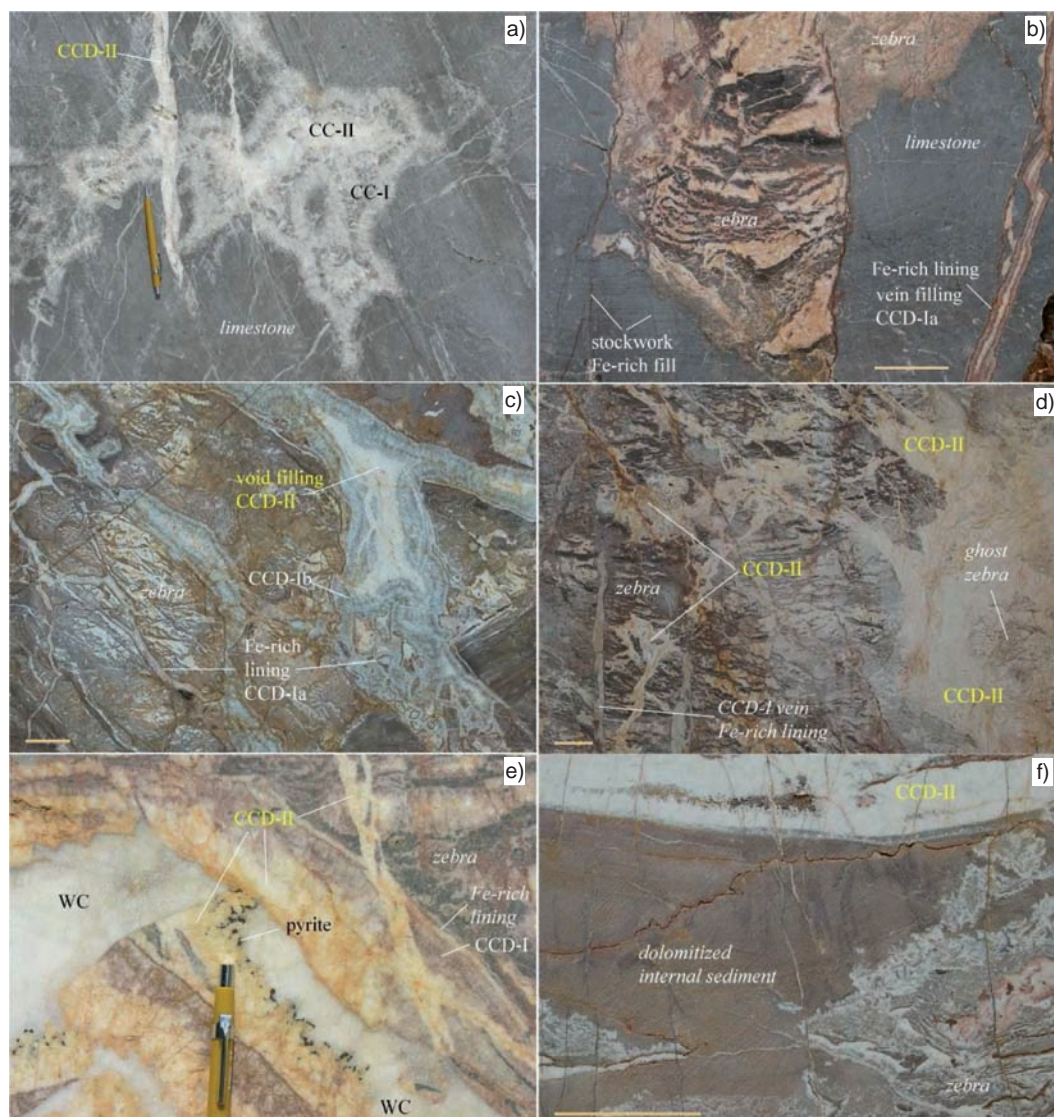


Figure 9

Paragenetic sequence of cements, Pozalagua Quarry. a) Cavity filling calcites (CC-I, CC-II) cut by non ferroan dolomite (CCD-II), quarry floor; note that CCD-II does not replace the limestone; b) Fe-rich dolomite stockwork, CCD-I vertical vein and coeval zebra, quarry top level; c) Large cavities filled by CCD-I precipitates in host zebras, plugged by CCD-II, NE corner; d) CCD-II (non ferroan) dolomites invading and replacing zebras, northern wall; note the older vertical CCD-I vein with its distinctive brown rim and the non-symmetrical shape of CCD-II veins, suggesting replacement; e) Pyrite and White Calcite (WC) cementing fractured dolomite (CCD-I, CCD-II veins), northern wall; f) Layered dolomite (internal sediment) in pockets hosted in CCD-II. Scale bar is 20 cm long.

are composed of two substages: an early one (CCD-Ia), which includes a centimetre- scale rim of brown (Fe-rich) saddle dolomite – usually preferentially calcitised (see below); and a later grey to beige saddle dolomite cement with moderate Fe content (CCD-Ib). CCD-Ia is present as a cement in a dense network of veins in the Ranero limestone and as symmetrical linings of fractures and breccias (Fig. 9b), while CCD-Ib is seen, predominantly, as a precipitate in the largest cavities only (Fig. 9c);

- non-ferroan dolomite cements (CCD-II) are composed of coarse white saddle crystals, often lacking systematic orientation, but plugging cavities lined by CCD-Ib, or in independent decimetre-scale veins cutting massive CCD-I and/or limestones (Fig. 9d);
- pyrite deposition followed by white coarse calcite (WC) that is precipitated in the central void spaces of CCD-I or CCD-II (Fig. 9e), and as decimetre veins cutting across.

At this stage, it is worth noting that dolomite is also present as a replacement product of limestone linked to CCD-I (ferroan, *Fig. 9b*), as a separate cement phase in zebras – which are also invaded by CCD-II (non ferroan, *Fig. 9d*) –, and in pockets of layered, pink sucrosic rocks interpreted as dolomitized internal sediments of the pre-hydrothermal cave system (*Fig 9f*).

The sequence of cements – listed above – may be found filling up the same structures or, alternatively, as cross-cutting veins, thus suggesting that the fluids followed new pathways at each stage while still reusing the previous ones. A formerly mined vein containing coarse white calcite, galena, and barite within ferroan dolomite (described in Herrero, 1989) is found cutting across the slope carbonate next to the Pozalagua Quarry. Besides, the deposition of clear, honey-colour calcite (TC), not included in the sequence of hydrothermal phases (listed above), is considered to represent the latest diagenesis cementation event, and is found in the form of pore-fillings and dedolomitization (calcitization and oxidation) of the most unstable dolomites (mainly CCD-Ia).

### 3.2.2 Geochemical Attributes

As previously reported in López-Horgue *et al.* (2010), successive hydrothermal cements have distinctive isotopic and chemical characteristics (*Fig. 10*). All these cements have low to very low  $\delta^{18}\text{O}$  values (with respect to the original, Albian seawater signature), suggesting precipitation from hot fluids. Besides,  $\delta^{18}\text{O}$  values show a decreasing trend along the sequence from CC-I and CC-II (–10 to –12‰) to CCD-I (–12 to –16‰), CCD-II (–17 to –19‰) and WC (–16 to –18‰). Host limestones show variably depleted  $\delta^{18}\text{O}$  values, probably suggesting that the fluids flowed through the limestones – downflow of the limestone-dolomite front – and were abundant enough to shift their oxygen signatures over a relatively large magnitude.  $\delta^{13}\text{C}$  of hydrothermal precipitates cluster in a narrow range (0 to +2‰) which is slightly, but consistently lower than its limestone counterpart (+1.5 to +3‰). This may indicate that some external carbon was brought by the fluids to produce the calcite and dolomite precipitates. Another likely explanation relates to the weak temperature fractionation effect on  $\delta^{13}\text{C}$  (*i.e.* 0.03 per °C; Emrich *et al.*, 1970). Limestone  $\delta^{13}\text{C}$  signatures cannot be distinguished from original values and those of marine cements as reported in Rosales and Perez-Garcia (2010).

Dedolomitization involves calcite showing low  $\delta^{13}\text{C}$  values coupled with relatively heavy  $\delta^{18}\text{O}$  values, invoking a telogenetic origin (TC, *Fig. 10a*). This calcite cement phase (TC; honey-colour, see above) marks the end-member of partially calcitized dolomites (dedolomites) along a  $\delta^{13}\text{C}$ -depletion,  $\delta^{18}\text{O}$ -increasing trend (*Fig. 10a*).

The Fe and Mn contents of hydrothermal dolomites show clusters that correlate well with their  $\delta^{18}\text{O}$  values (*Fig. 10b, c*). For CCD-Ia and CCD-Ib ferroan dolomites, FeO contents

cluster around 1-1.5% and 0.5-0.7%, respectively. CCD-II dolomites have very low FeO contents (<0.2%). Altogether, the more Fe-rich dolomites (CCD-Ia) have the less depleted oxygen isotope ratios, and the Fe-poor dolomites (CCD-II) the most depleted oxygen isotopes ratios. It should be noticed, however, that the contents of FeO and MnO in Figures 10b and c represent averaged values obtained from microdrillings of plugs.

Microprobe analyses of CDD-I dolomites (*Fig. 10d*) reveal a wider range of Fe contents and some (limited) departure from stoichiometry. Some CCD-Ia dolomites contain up to 1.7%  $\text{FeCO}_3$  (Fe-rims) and 55% molal  $\text{CaCO}_3$ , but these compositions are unstable in late (oxidizing) fluids, so they are rarely preserved and frequently converted to calcite (TC) and Fe-Mn hydroxides during telogenetic alteration (*e.g.* dedolomitization).

The carbon and oxygen isotope ratios of replacive dolomites are similar to those of hydrothermal precipitates, so they can be linked to stages CCD-Ia, Ib or CCD-II on the basis of decreasing  $\delta^{18}\text{O}$  values and decreasing Fe content. However, the Fe content of replacive dolomites may be substantially larger than that of the present-day Fe content of their exclusive carbonate fraction; this simply confirms that their mineralogy includes pyrite and/or silicates in addition to dolomite, and that the corresponding rocks have a multi-stage history.

### 3.2.3 Back-Scatter SEM and Major/Trace Element Composition

Hydrothermal precipitates (or cements) have a diagnostic symmetrical structure (*Fig. 11a*) and a very low level of silicate impurities ( $\text{Al}_2\text{O}_3$  typically less than 0.05 wt%; *Fig. 11b*). CC-I, CC-II and WC are such precipitates, while TC mostly appears to have been formed, later on, both as a replacement product of unstable Fe-dolomite and as cement in pores (in a telogenetic realm). All dolomite cements are subidiomorphic (anhedral/nonplanar) and have curved crystal shapes (saddle) (*Fig. 11c, d*). In some cases the full compositional range (CCD-Ia to CCD-II) is seen in one single zoned crystal. Internal (central) porosity is free or plugged by WC and/or TC phases. Replacive dolomites are best identified by their mosaic textures and/or by their higher content in silicate impurities. The replacive (dark) bands of zebras typically have a higher  $\text{Al}_2\text{O}_3$  content (0.1-0.3%) (*Fig. 11b*) than those of the corresponding (void filling) white bands (<0.1%). Dolomites with a layered macroscopic structure (*Fig. 9f*) have the highest content of non-carbonate impurities ( $\text{Al}_2\text{O}_3$  up to 1.5%). Since these impurities are essentially of clayey origin (see also Shah *et al.*, this volume), we interpret these particular rocks as former clay-bearing sediments that accumulated in ponds of the pre-hydrothermal cave system and were later converted to dolomite together with the surrounding limestones.

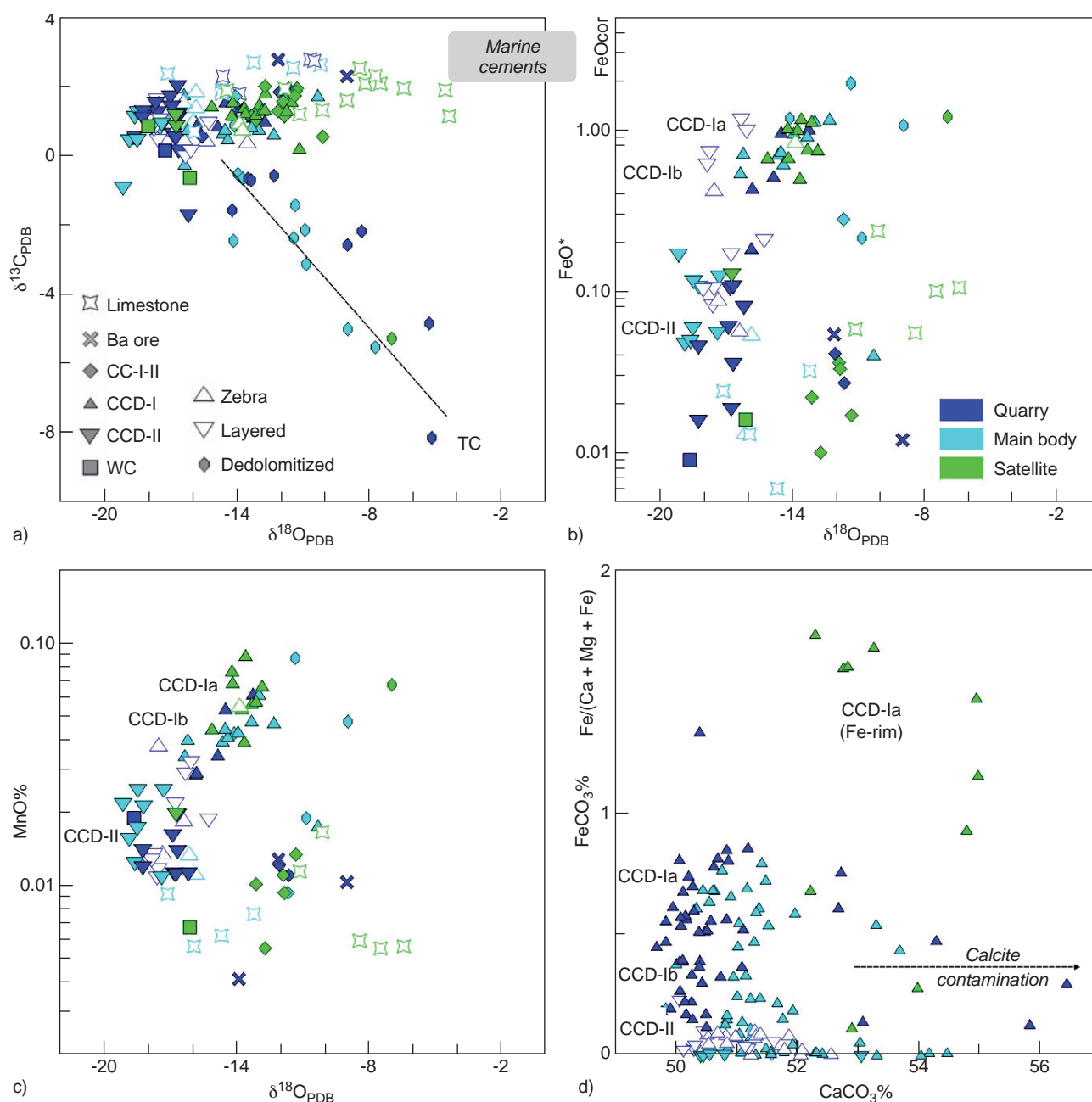


Figure 10

Geochemical attributes of limestones, cements and replaced rocks. Samples are classified as a function of paragenetic stage for minerals (filled symbols) or lithotype for rocks (open symbols). Colours refer to sampling locations: the Quarry stands for the stratigraphically deepest outcrops (road breccia and quarry), main body for the upper levels (fault and plateau), and satellite for a vein body (about one kilometer east of Pozalagua quarry). a-c) Data from microdrills or whole rocks; d) Microprobe data. The FeO content of carbonate ( $FeO^*$  wt%) is estimated by correcting the bulk Fe content from a silicate contribution having the same Fe/Al ratio as claystone.

Dolomite crystal sizes of replaced rocks increase as their FeO content (and  $\delta^{18}O$ ) decreases. Replaced limestones lacking zebra texture have the smallest grain size (tens of microns) and rocks reworked by CDD-II fluids the highest (millimetres).

All replacive dolomites, however, have curved crystal shapes and are subidiomorphic (sub- to anhedral). Interestingly, the non-carbonate paragenesis varies with the hydrothermal stage, with illite  $\pm$  kaolinite at stage CCD-I (*cf. Fig. 11b*) and

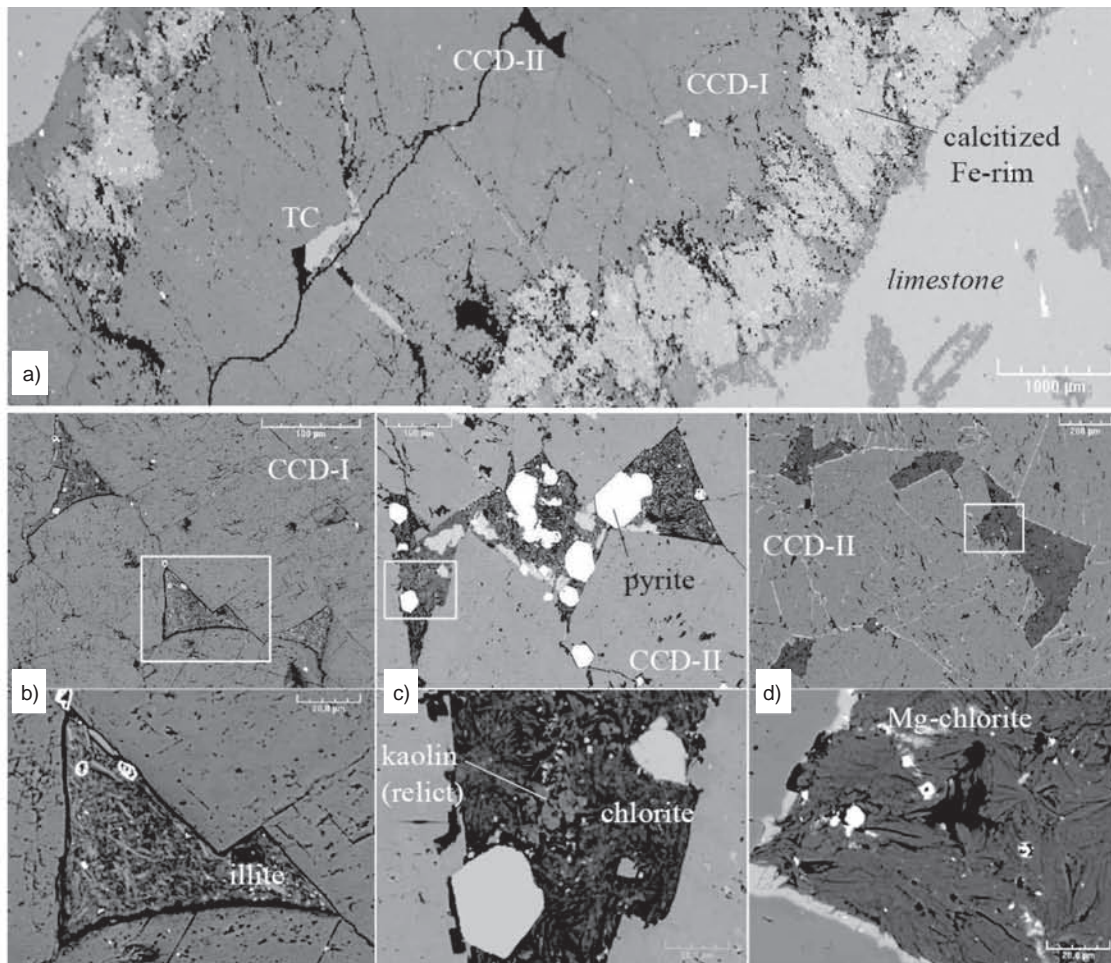


Figure 11

BSE images of hydrothermal precipitates and replacive dolomites. a) Composite vein cutting across the limestones, road breccia. Note the symmetrical structure of vein fillings, the incipient dolomitization of limestone, and the selectively dedolomitized Fe-rich rim. b) Dark band in zebra dolomite. c, d) Dolomitized internal sediments, Pozzalagua Quarry. Note the idiomorphic contour of dolomite crystals against silicates.

Mg-chlorite at stage CCD-II (*cf. Fig. 11c, d*); quartz is typically absent.

### 3.3 Petrophysical Analyses

The host rock, which is a tight limestone, is characterized by very low porosity (<0.5%) and permeability values (0.01 mD). HTDs are characterized by a much wider range of porosity and permeability values. No clear porosity/permeability relationship trend could be drawn from the produced data set in the Ranero main dolomite body. Porosity values range from 1.8 to 12.1% and the average is 5.7%; while permeability values vary between 0.01 and 17.42 mD and have an average of 1.1 mD. It can thus be concluded that the dolomitization had a positive effect on the reservoir properties

of the altered host rock. Both porosity (*Fig. 6*) and permeability (*Fig. 7*) values in the Pozzalagua (Ranero) HTD Body, show clusters of high and low values.

The investigated HTD can be divided in three classes based on their texture and different pore types (*Fig. 12*):

- matrix dolomite;
- dolomite cement;
- zebra dolomite.

First, the dark grey matrix (fine crystalline) dolomite is characterized by subhedral, small dolomite crystals and small rounded pores with a diameter less than 3 μm (*Fig. 12a, b*). These dolomites have porosity values ranging from 5 to 11.8% with an average of 6.8%. Permeability values occur in a broad range and are between 0.03 and 17.4 mD and the average permeability is 2.3 mD.

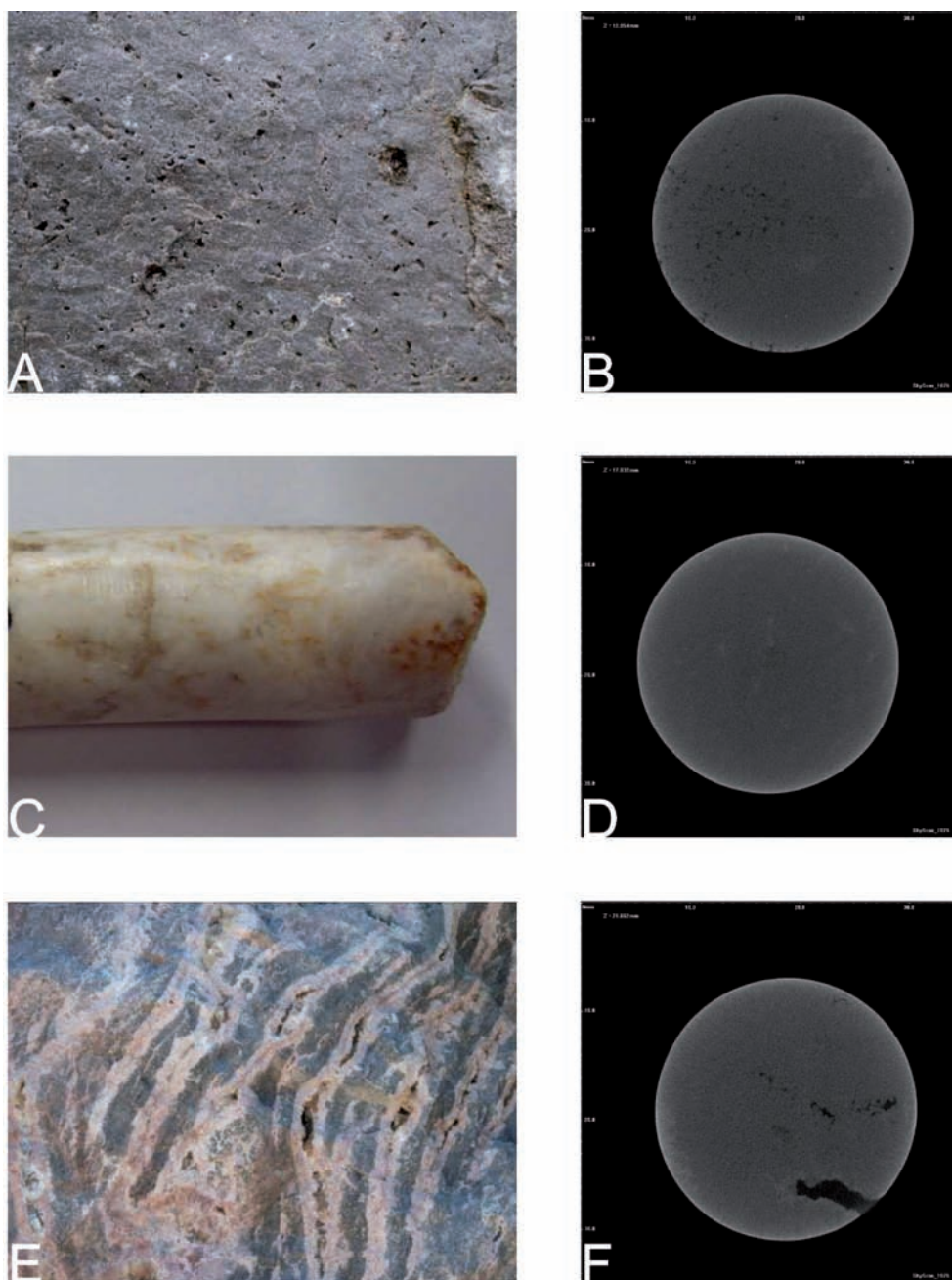


Figure 12

Overview of the main dolomite types (based on their texture and pore type). a) Matrix dolomite, characterized by dark grey, fine crystalline dolomite. b)  $\mu$ CT scan showing the presence of small pores in matrix dolomites. c) Coarse crystalline cement dolomite. d)  $\mu$ CT scan of cement dolomite shows the relatively tight character of the dolomite type. e) Zebra dolomite consisting of alternating layers of fine crystalline, dark and coarse crystalline, light dolomite. f)  $\mu$ CT scan of a zebra dolomite showing the presence of aligned and closely spaced pores ( $\sim 1$  cm).

CCD-I & II dolomite cements (irrespective of Fe-content) are represented by coarse crystalline pink to white dolomite crystals, generally anhedral with sweeping extinction. They are characterized by bladed crystals with saddle morphology.

Pores are intercrystalline to vuggy (*Fig. 12c, d*). Cement dolomites have porosities ranging between 1.9 and 11.7%, with an average of 5.8%. Permeability values are between 0.01 and 10.3 mD, with an average of 1 mD.

Zebra dolomites are from a textural point of view built up by alternating layers of matrix dolomite and cement dolomite in an ABBA arrangement (Vandeginste *et al.*, 2005). Pores are generally elongated and occur between two layers of cement dolomite (Fig. 12e, f). Zebra dolomites frequently occur and are characterized by porosity values between 1.8 and 12.1% with an average porosity of 5.5%. Permeability values are between 0.01 mD and 16.8 mD, the average is 1 mD.

## 4 DISCUSSION

The Ranero HTD case study features mainly two distinct phases of hydrothermal dolomitization and two minor phases of hydrothermal calcite deposition along fluid pathways controlled by palaeo- and hypogene karstification, fracturing and brecciation. Perhaps the most remarkable aspect of this case study is that the first dolomitizing phase is a ferroan one (CCD-I), while the second is non-ferroan (CCD-II), both being precipitated at relatively high temperature as suggested by the very negative  $\delta^{18}\text{O}$  values (down to  $-19\%$  V-PDB) and by fluid inclusion homogenization temperatures (López-Horgue *et al.*, 2010). This sequence is less commonly observed in HTDs (Davies and Smith, 2006) or MVT deposits (Leach *et al.*, 2005), as the dolomites are usually Fe-rich during the whole dolomitization. Besides, the early ferroan phase at Ranero appears to have the highest regional extent – as it is found and documented at several sites in the vicinity – while the later non-ferroan one seems to be more abundant in the vicinity of the Pozalagua Fault. A few kilometers away from Ranero, where the same two dolomite stages are reported, the first (ferroan) stage is associated with some Zn-Pb sulfides (Shah *et al.*, this volume).

Enlarging the picture to the Basque-Cantabrian Basin (BCB) and its ore geology, the Ranero case can be viewed as a high temperature, Fe-poor end-member within a large variety of carbonate-hosted Fe-Zn-Pb deposits: the opposite end-member is represented by the relatively lower temperature – and very Fe-rich – La Troya deposit (Velasco *et al.*, 1994), and intermediate members include typical MVT deposits such as Reocín (Velasco *et al.*, 2003) and perhaps Ixtaspe (Piqué *et al.*, 2009). Note that in this picture the Bilbao Fe-carbonate ores (*e.g.*, Simon *et al.*, 1999), which are both Fe-rich and record rather high fluid inclusion temperatures, are set apart because they are hosted in shallow marine limestones. Considering the overall similarity of Ranero's dolomites with HTDs and HTD hosted MVT deposits, their genesis raises essentially the same questions which are briefly discussed hereafter, *i.e.*:

- how did the fluids migrate and why were they focused along the platform edge and;
- what chemical composition is characteristic of the dolomitizing fluids, and why did they react with the host carbonates?

However, several differences compared to the “archetypal” HTD's sequence as proposed by Davies and Smith (2006) may question some aspects of the currently accepted models and suggest some new genetic schemes.

### 4.1 Geometry, Fluid Pathways and Fluid Drives

An important aspect of the Ranero case, which fits only superficially the “archetypal” HTD is the association with palaeo- and hypogene karstification. Here, it must be noted that this type of karstification differs from the early meteoric karst features that were previously described by López-Horgue *et al.* (2010) and Kurz *et al.* (2011). The early phase of dolomite precipitation clearly post-dates this hypogene dissolution phases and earlier calcite fillings (CC-I and CC-II) that precipitated at relatively high temperatures (Fig. 9a, 10a). The volume of dolomite is significant in the Pozalagua Quarry, and this is likely due to the large development of pre-hydrothermal fracture and dissolution-enhanced voids. Since internal sediments, such as frequently reported in MVT deposits (Kendal, 1960), need a large network of void space to form, we suggest that void-forming processes in the present case are preliminary rather than a consequence of HTD forming processes.

From a structural point of view, pre-hydrothermal dissolution is seemingly controlled by surface proximity (and unconformities) and the development of vertical strike-slip faults. Anchoring vertical structures on these weak zones, and perhaps on deeper structures, is believed to generate and to maintain potential fluid pathways breaching the edge of the platform carbonates (*cf.* Fig. 4b). This provides, therefore, a connection with the basinal shales and with deep-seated horizons (potential aquifers) (López-Horgue *et al.*, 2010). Although this is not the only possibility, we suggest that this particular geometry enables the Ranero Fault (and its nearby faults) to represent realistic escape pathways, both for fluids released by compaction of the basinal shales and for fluids stored in deep aquifers (and potentially below the platform as well). Moreover, such a hydraulic connectivity may ultimately result in pressure buildups (driven by shale compaction) along the whole pathway until the carbonate undergoes dilational fracturing and the top seal is breached.

The Ramales Platform carbonates were indeed adjacent to a basin that has been the depocenter of some 7 000 m of sediments (mostly siliciclastics; Fig. 4b) which have been relatively rapidly deposited during the Albian (López-Horgue *et al.*, 2010). During burial, compaction dewatering processes must have driven a large quantity of marine-derived waters along the few possible escape routes. Alternatively, fluids may have been moving in response to gravity (salinity) gradients from the platform side or as a consequence of heat anomalies (convection) inside the platform or along its edge. Potential

sources of heat anomalies (temperature gradients) are quite numerous, including:

- the Keuper diapiric deformation (*e.g.* Canérot *et al.*, 2005);
- the differential subsidence along the platform border;
- the strike-slip movements themselves, ultimately related to crustal thinning (López-Horgue *et al.*, 2010).

Altogether, the fluid drives are not well constrained in the Ranero case, but the capacity of the system to focus fluid flow along pathways transverse to the edge of the platform remains the most remarkable aspect.

Furthermore, the two dolomitization episodes and the associated hydrothermal events are believed to have occurred during the Late Albian, as they are pre- and post-dated by bed-parallel stylolites (Swennen *et al.*, in press). López-Horgue *et al.* (2010) proposed a latest Albian-Turonian age for the hydrothermal dolomitization in the studied area constrained by stratigraphical, structural and burial analyses. This fact does not refute that minor mineralisation (including dolomitization) events did occur during later tectonic stages of the basin (*e.g.* compression and inversion in the Late Cretaceous to Eocene), but not the observed pervasive dolomitization.

## 4.2 Fluid Chemistry and Reaction Drives

The very first episode (Fe-rich) CCD-Ia developed an extended stockwork of veinlets over the whole Ranero main body. Albeit this distribution is reminiscent of hydraulic (dilatational) fracturing and overpressure, it does not imply large fluid fluxes. In fact, much of the following CCD-Ib dolomites actually replace limestone. The coeval mass transfer requires much larger fluid fluxes and sustained fluid undersaturation with respect to calcite. Interestingly, the replacement of early hydrothermal calcite (CC-II) by CCD-Ib dolomite is well exposed in the satellite body (also called vein-body; Fig. 8a). The newly formed dolomites have a particular texture and form a palisade of plumose, decimetre scale crystals. The mere fact that CC-II calcites are very coarse, hence they offer very low reactive surface to dolomitizing fluids, explains simply why their dolomitization is very difficult, so it appears in the field as a relict calcite dyke (*cf.* Fig. 8b) engulfed in CCD-Ib dolomite.

The CCD-II veins are, usually, nearly straight and small (centimeter to decimeter scale) when hosted in the limestone (Fig. 9a), while they expand to the metre-scale and develop irregular limits when entering the CCD-I dolomite body in the Pozalagua Quarry. Therefore, they do not seem to pervasively replace limestone in the Pozalagua Quarry, but rather replace previous CCD-I dolomites (including the zebras). Another (chemical) argument for such a replacement is that some dolomites have mineral compositions characteristic of a second stage (Fe-poor) and highly depleted  $\delta^{18}\text{O}$  values (CCD-II) while the bulk rock Fe content is typical of stage

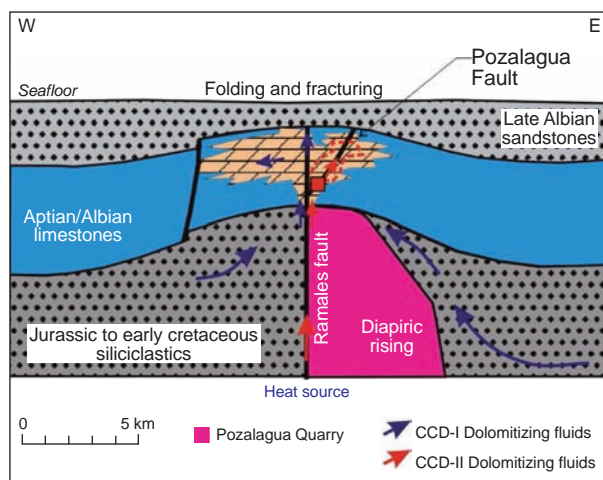


Figure 13

Schematic representation of the dolomitization model for the Ranero area (after López-Horgue *et al.*, 2010) featuring conceptually the flow paths of the pervasive, ferroan (compactional) CCD-I and localized non-ferroan (diaper-associated) CCD-II dolomitizing fluids.

CCD-I: the excess Fe is hosted in (oxidized) pyrite and it is interpreted as inherited from a CCD-I dolomite being converted to CCD-II (+ pyrite).

From a geochemical viewpoint, these features suggest that most CCD-I related fluids should be acidic and Mg-rich, promoting limestone replacement (Fig. 13). Moreover, they should not be  $\text{H}_2\text{S}$ -rich in order to allow the transport of reduced Fe and Mn. These are frequently advocated properties of MVT ore fluids. On the contrary, the genesis of non-ferroan CCD-II dolomites does not require the fluids to be acidic (as they do not dissolve calcite) or particularly Mg-rich (as they mostly replace previous Fe-dolomite). CCD-II related fluids are obviously Fe poor. Given that this second stage ends with some pyrite deposition, a likely possibility is that the corresponding fluids were rich in reduced sulphur ( $\text{H}_2\text{S}$ ,  $\text{HS}^-$ ) and thus almost unable to transport Fe. We emphasize that highly reduced sulphur content could invoke the reaction of CCD-II fluids with all Fe-bearing minerals (including Fe dolomite and silicates) to produce Fe-poor dolomite, Mg-chlorite and pyrite. The suggested chemical contrast between early (ferroan) and late (non-ferroan) dolomitizing fluids is reminiscent of that advocated for Australian Proterozoic sedex deposits (Cooke *et al.*, 2000) between oxidized (MVT-like) and reduced brines, although the inferred pH characteristics may be quite different. This chemical contrast and the inferred high fluid temperatures give permissive evidence for a somewhat new genetic scenario.

### 4.2.1 CCD-I Dolomitizing Fluids

Mg-rich fluids (CCD-I) likely originated as sulphate-dominated marine waters. This fits with compactional waters or marine

waters mixed with ancient (stored) aquifer brines. In order to increase their acidity, such fluids need to be heated – being driven towards a hot zone or mixed with hot fluids – (Fig. 13), and undergo localized sulphate reduction (TSR) with their own content of local reductant source (organic matter, oil or gas). The fact that the fluids became acidic is crucial for pervasive dolomitization, because Mg-rich fluids which gained acidity are prone to coupled limestone dissolution and precipitation of dolomite. It should be noticed that, whatever the ultimate origin of the fluids (either cold or hot), the sulfate (and Mg) and the reducing agent are supposed to meet in a hot siliciclastic host. This may apply to compactional fluids, as they can be expelled towards the platform edge area at a moment when a temperature anomaly occurs due to differential subsidence and faulting linked to crustal stretching processes (García-Mondéjar *et al.*, 2004b; López-Horgue *et al.*, 2010). Note also that the compactional fluid drive provides a simple explanation for pressure buildups and related pulses of overpressure relaxation (expressed by dilational jointing and brecciation) as observed for CCD-I.

#### 4.2.2 CCD-II Dolomitizing Fluids

The origin of the fluids that precipitated the non-ferroan dolomites (CCD-II) is seemingly different, or at least their history involved different steps. If these fluids gained the needed H<sub>2</sub>S from TSR, they must have been buffered to lose their capacity to react with calcite before invading the Ranero Fault system (Fig. 13). The iron poor carbonate platform limestones may have buffered the fluid acidity. To follow this path, the fluids should pass through a TSR prone, hot zone that is most probably located within the interior platform. The ultimate origin of the sulphate is less constraining, as the corresponding fluids are not necessarily Mg-rich and evaporitic sulphate (Hanor, 1994) can be invoked as well. In this scenario, the Pandra Diapir, which is at the intersection of the Ramales and Cabuérniga Faults (Fig. 5) and underlies the Ranero area, could have acted both as a source of sulphate and as the core of a thermal anomaly owing to the salt conductivity. Similar diapirism and associated structural effects have been recorded in the coeval hydrothermally dolomitised reservoirs in Aquitaine (France; Canérot *et al.*, 2005). We, thus, suggest that convective flow above a salt diapir and subsequent TSR within a limestone host may provide the right conditions to generate CCD-II fluids. If this model is correct, it is important to emphasise that the resulting fluids lose very soon their capacity to react with calcite, hence their effects may be difficult to detect in the platform carbonates. Conversely, they should react with any Fe-bearing lithology (including Fe-dolomite) to precipitate pyrite. The implication is that a rock record of these fluids should be searched for along the contacts between platform carbonates and the surrounding siliciclastics, under the form of pyritization halos around the veins emerging from the carbonates.

## CONCLUSIONS

Regional stratigraphic and structural factors prevailing through the Albian, resulted in the development of a deep basin with thick sedimentary pile (troughs in the Basque-Cantabrian Basin, BCB) adjacent to a carbonate platform (the Ramales Platform), which was undergoing local folding, faulting and deformation due to diapirism.

Pre-hydrothermal and hypogene karstification along faults generated fluid pathways across the platform margin. This karstification was succeeded by the precipitation of hydrothermal calcite, various stages of dolomitization, hydraulic fracturing, brecciation, limestone replacement and a late stage of calcite precipitation.

Dolomitization at Ranero is associated with two main stages of hot (150-200°C) fluid migration, that caused increasingly <sup>18</sup>O depleted dolomites (from –10.5 to –18.7‰ V-PDB), with decreasing Fe contents and different authigenic mineral associations (illite and kaolinite *versus* Mg-chlorite; Shah *et al.*, this volume). While these characteristics point towards substantial changes in the chemistry of the successive fluid pulses, the system evolved from producing, regionally distributed HTD bodies dominated by zebras and limestone replacement, towards narrower and more local dolomite veins reworking the previous ones, with little apparent replacement of the host limestones.

Although the regional-scale mechanism of HTD (seemingly related to compactional fluids) may explain enhanced reservoir properties during dolomitization with respect to the original limestone, the second, non-ferroan dolomite phase seems to decrease the pre-existing porosity. At the scale of an HTD geobody, the successive dolomitising phases generate significant reservoir heterogeneities that seem to be inherently related to the mechanism of dolomitization, fluid chemistry and reaction drives.

## ACKNOWLEDGMENTS

This contribution consists of a group-work involving various academic and industrial groups which have been studying the dolomite features that are exposed in the Ranero area (northern Spain). These groups include the University of Basque Country, Spanish Research Council (CSIC), TOTAL, IFP Energies nouvelles (France), Statoil, the Katholieke Universiteit Leuven (Belgium), and Saint-Étienne School of Mines (France). The idea of writing up a common paper has emerged from a workshop that was held at IFP Energies nouvelles on the 31st of May and 1st of June, 2010, devoted to the hydrothermal dolomites of Ranero and nearby regions in Cantabria and the Basque Country. During this workshop, it was agreed to present a joint-paper aiming at consolidating a common conceptual model for the Ranero hydrothermal dolomites. The authors would like to thank their academic and industrial institutions for allowing them to publish some

results of their research work. Critical reviews and valuable comments from anonymous referees have helped in improving the presentation and content of this contribution and are greatly appreciated.

## REFERENCES

- Berger Z., Davies G.R. (1999) The development of linear hydrothermal dolomite (HTD) reservoir facies along wrench or strike-slip fault systems in Western Canada sedimentary basin, *Canadian Society of Petroleum Geologists Reservoir*, January, **26**, 34-38.
- Boillot G., Malod J. (1988) The north and north-west Spanish continental margin: a review, *Revista de la Sociedad Geológica de España* **1**, 3-4, 295-316.
- Caline B., Sudrie M., López-Horgue M.A., Fernández Mendiola P.A., Iriarte E. (2006) Fault-related hydrothermal dolomites of Cretaceous platform carbonates outcropping in the Karrantza area (North Spain): lessons learned for a better characterisation of sub-surface dolomite reservoirs, in *17th International Sedimentological Congress*, Fukuoka, Japan.
- Canérot J., Hudec M.R., Rockenbauch K. (2005) Mesozoic diapirism in the Pyrenean orogeny: Salt tectonics on a transform plate boundary, *AAPG Bull.* **89**, 2, 211-229.
- Cantrell D.L., Swart P.K., Hagerty R.M. (2004) Genesis and characterization of dolomite, Arab-D Reservoir, Ghawar Field, Saudi Arabia, *GeoArabia* **9**, 11-36.
- Conliffe J., Azmy K., Gleeson S.A., Lavoie D. (2010) Fluids associated with hydrothermal dolomitization in St. George Group, western Newfoundland, Canada, *Geofluids* **10**, 422-437.
- Cooke D.R., Bull S.W., Large R.R., McGoldrick P.J. (2000) The importance of oxidized brines for the formation of Australian Proterozoic stratiform sediment-hosted Pb-Zn (Sedex) deposits, *Econ. Geol.* **95**, 1, 1-18.
- Davies G.R., Smith Jr L.B. (2006) Structurally controlled hydrothermal dolomite reservoir facies: An overview, *AAPG Bull.* **90**, 11, 1641-1690.
- Dewit J., Swennen R., Muechez Ph., Huysmans M., Hunt D., Thurmond J. (2009) Geometry, distribution and characteristics of hydrothermal dolomite (HTD) bodies hosted by an Aptian-Albian carbonate platform, Basque-Cantabrian Basin, northern Spain, *27th IAS meeting of Sedimentology*, 151.
- Dewit J., Foubert A., Claes S., Huysmans M., Muechez Ph., Hunt D., Swennen R. (2010) Parameters influencing the reservoir characteristics of hydrothermal dolomite (HTD) bodies in back-reef and inner-platform carbonates, a case study from Ranero and Bueras (northern Spain), *18th International Sedimentology Congress*, 299.
- Dickson J.A.D. (1966) Carbonate identification and genesis as revealed by staining, *J. Sediment. Petrol.* **36**, 491-505.
- Emrich K., Ehhalt D.H., Vogel J.C. (1970) Carbon isotope fractionation during precipitation of calcium carbonate, *Earth Planet. Sci. Lett.* **8**, 363-371.
- García-Mondéjar J., Agirrezabala L.M., Aranburu A., Fernández-Mendiola P.A., Gómez-Pérez I., López-Horgue M., Rosales I. (1996) Aptian-Albian tectonic pattern of the Basque-Cantabrian Basin (northern Spain), *Geol. J.* **31**, 13-45.
- García-Mondéjar J., Fernández-Mendiola P.A., Agirrezabala L.M., Aranburu A., López-Horgue M.A., Iriarte E., Martínez de Rituerto S. (2004a) El Aptiense-Albiense de la Cuenca Vasco-Cantábrica, in *Geología de España*, Vera J.A. (ed.), SGE-IGME, Madrid, pp. 291-296.
- García-Mondéjar J., Fernández-Mendiola P.A., Agirrezabala L.M., Aranburu A., López-Horgue M.A., Iriarte E., Martínez de Rituerto S. (2004b) Extensión del Aptiense-Albiense en la Cuenca Vasco-Cantábrica, in *Geología de España*, Vera J.A. (ed.), SGE-IGME, Madrid, pp. 340-343.
- García-Mondéjar J., López-Horgue M.A., Aranburu A., Fernández-Mendiola P.A. (2005) Pulsating subsidence during a rift episode: stratigraphic and tectonic consequences (Aptian-Albian, northern Spain), *Terra Nova* **17**, 517-525.
- Hanor J.S. (1994) Origin of saline fluids in sedimentary basins, in *Geofluids: Origin and Migration of Fluids in Sedimentary Basins*, J. Parnell (ed.), *Geol. Soc. London Spec. Publ.* **78**, 151-174.
- Herrero J.M. (1989) Las mineralizaciones de Zn, Pb, F en el sector occidental de Vizcaya: Mineralogía, geoquímica y metalogénia, *Doctoral Thesis*, Universidad del País Vasco, 285 pp.
- Iriarte E., López-Horgue M.A., Schröder S., Fernández-Mendiola P.A., Caline B. (2009) Zebra-dolomite, tectonic deformation and hydrothermal fluid-flow: lessons learned from Asón valley hydrothermal dolomites (northern Spain), *27th IAS Meeting of Sedimentology*, Alghero, Italy, Abstract Book, p. 217.
- Kendall D.L. (1960) Ore deposits and sedimentary features, Jefferson City Mine, Tennessee, *Econ. Geol.* **55**, 5, 985-1003.
- Kurz T.H., Dewit J., Buckley S.J., Thurmond J.B., Hunt D.W., Swennen R. (2011) Hyperspectral image analysis of different carbonate lithologies (limestone, karst, hydrothermal dolomites): the Pozalagua Quarry case study (Cantabria, NW Spain), *Sedimentology* (under reviewing).
- Leach D.L., Sangster D.F., Kelley K.D., Large R.R., Garven G., Allen C.R., Gutzmer J., Walters S. (2005) Sediment-hosted lead-zinc deposits: a global perspective, *Econ. Geol.* 100th Anniversary Special Volume, 561-607.
- López-Horgue M.A. (2000) El Aptiense-Albiense de Karrantza-Lanestona (Bizkaia y Cantabria), *PhD Thesis*, Universidad del País Vasco, Euskal Herriko Unibertsitatea, 264 pp., Unpublished.
- López-Horgue M.A., Aranburu A., Fernández-Mendiola P.A., García-Mondéjar J. (2000) Existencia de una discordancia angular con laguna de Albiense medio en el Complejo Urgoniano de Ranero (Ramales-Karrantza, región vasco-cantábrica), *Geogaceta* **28**, 89-92.
- López-Horgue M.A., Fernández-Mendiola P.A., Iriarte E., Sudrie M., Caline B., Gomez J.P., Corneillie H. (2005) Fault-related hydrothermal dolomite bodies in early Cretaceous platform carbonates, Karrantza area (North Spain): outcrop analogs for dolomite reservoir characterization, in *10<sup>e</sup> Congrès français de sédimentologie*, Presqu'île de Giens, France.
- López-Horgue M.A., Owen H.G., Aranburu A., Fernández-Mendiola P.A., García-Mondéjar J. (2009a) Early late Albian (Cretaceous) of the central region of the Basque-Cantabrian Basin, northern Spain: biostratigraphy based on ammonites and orbitolinids, *Cretac. Res.* **30**, 385-400.
- López-Horgue M.A., Iriarte E., Schroder S., Fernández-Mendiola P.A., Caline B. (2009b) An example of the tectonic origin of zebra dolomites: the San Martín beach outcrop (Santoña, North Spain), *Geogaceta* **47**, 85-88.
- López-Horgue M.A., Iriarte E., Schroder S., Fernández-Mendiola P.A., Caline B., Corneillie H., Fremont J., Sudrie M., Zerti S. (2010) Structurally controlled hydrothermal dolomites in Albian carbonates of the Asón valley, Basque Cantabrian Basin, Northern Spain, *Mar. Petrol. Geol.* **27**, 5, 1069-1092.
- Nader F.H., Swennen R., Ellam R. (2004) Reflux stratabound dolostone and hydrothermal volcanism-associated dolostone: a two-stage dolomitization model (Jurassic, Lebanon), *Sedimentology* **51**, 339-360.
- Nader F.H., Swennen R., Ellam R. (2007) Field geometry, petrography and geochemistry of a dolomitized front (late Jurassic, central Lebanon), *Sedimentology* **54**, 1093-1119.

- Nielsen P., Swennen R., Muechez Ph., Keppens E. (1998) Origin of Dinantian zebra dolomites south of the Brabant-Wales Massif, Belgium, *Sedimentology* **45**, 4, 727-743.
- Piqué A., Canals A., Disnar J.R., Grandia F. (2009) *In situ* thermochemical sulfate reduction during ore formation at the Itxaspe Zn-(Pb) MVT occurrence (Basque-Cantabrian basin, Northern Spain), *Geologica Acta* **7**, 431-449.
- Ronchi P., Jadoul F., Ceriani A., Di Giulio A., Scotti P., Orteni A., Previde Massara E. (2011) Multistage dolomitization and distribution of dolomitized bodies in Early Jurassic carbonate platforms (Southern Alps, Italy), *Sedimentology* **58**, 2, 532-565.
- Rosales I., Pérez-García A. (2010) Porosity development, diagenesis and basin modeling of a Lower Cretaceous (Albian) carbonate platform from northern Spain, *Geol. Soc. London Spec. Publ.* **329**, 317-342.
- Rosenbaum J., Sheppard S.M. (1986) An isotopic study of siderites, dolomites and ankerites at high temperatures, *Geochim. Cosmochim. Acta* **50**, 1147-1150.
- Simón S., Canals À., Grandia F., Cardellach E. (1999) Estudio isotópico y de inclusiones fluidas en depósitos de calcita y dolomita del sector oeste del Anticlinal de Bilbao y su relación con las mineralizaciones de Fe-Zn-Pb, *Boletín de la Sociedad Española de Mineralogía* **22**, 55-71.
- Schröder S., Rigaud S., Zerti S., Borgomano J., Caline B., Gomez J.P., Hennuy J., Iriarte E., Lamarche J., López-Horgue M., Sudrie M. (2008) Characterization of fault-related dolomites bodies from outcrop analogs: application to carbonate reservoirs, in *8th Middle East Geoscience Conference and Exhibition*, Bahrain. Conference Program, Abstract CD.
- Shah M.M., Nader F.H., Dewit J., Swennen R., Garcia D. (2010) Fault-related hydrothermal dolomites in Cretaceous carbonates (Cantabria, northern Spain): Results of petrographic, geochemical and petrophysical studies, *Bull. Soc. Géol. Fr.* **181**, 4, 391-407.
- Shah M.M., Nader F.H., Garcia D., Swennen R. 2012 Hydrothermal dolomites in the lower Cretaceous (Albian) platform carbonates (Karrantza valley, N.W Spain): Comparative studies of two sites, *Oil Gas Sci. Technol.* **67**, 1, 97-122.
- Sudrie M., Caline B., López-Horgue M.A., Fernández-Mendiola P.A., Iriarte E. (2006) Fault-related hydrothermal dolomites in Cretaceous platform carbonates from the Karrantza area (North Spain): outcrop analog for dolomite reservoir characterization, in *7th Middle East Geoscience Conference and Exhibition*, Bahrain. Conference Program, Abstract CD.
- Swennen R., Dewit J., Fierens E., Muechez P., Shah M.M., Nader F.H., Hunt D., Multiple dolomitization events along the Pozalagua Fault (Pozalagua Quarry, Basque-Cantabrian Basin), *Sedimentology* (accepted).
- Vandeginste V., Swennen R., Gleeson S.A., Ellam R.M., Osadetz K., Roure F. (2005) Zebra dolomitization as a result of focused fluid flow in the Rocky Mountains Fold and Thrust Belt, Canada, *Sedimentology* **52**, 5, 1067-1095.
- Velasco F., Herrero J.M., Gil P.P., Alvarez L., Yusta I. (1994) Mississippi Valley-type, sedex, and iron deposits in lower Cretaceous rocks of the Basque-Cantabrian basin, Northern Spain, in *Sediment-hosted zinc-lead ores*, Fontboté L., Boni M. (eds), Springer, Berlin, SGA Special Publication **10**, 246-270.
- Velasco F., Herrero J.M., Yusta I., Alonso J.A., Seebold I., Leach D. (2003) Geology and geochemistry of the Reocín zinc-lead deposit, Basque-Cantabrian basin, Northern Spain, *Econ. Geol.* **98**, 1371-1396.
- Vergés J., García-Senz J. (2001) Mesozoic evolution and Cainozoic inversion of the Pyrenean Rift, in *Peri-Tethys Memoir 6: Peri-Tethyan Rift/Wrench Basins and Passive Margins*, Ziegler P.A., Cavazza W., Robertson A.H.F., Crasquin-Soleau S. (eds), *Mém. Mus. Natn. Hist. Nat.* **186**, 187-212, Paris, ISBN: 2-85653-528-3.

*Final manuscript received in August 2011  
Published online in February 2012*